Journal of Neuroscience Research 65:139–149 (2001)

Molecular Organization of the Nodal Region Is Not Altered in Spontaneously Diabetic BB-Wistar Rats

Alexander A. Brown,[1] Theodore Xu,[1] Edgardo J. Arroyo,[1] S. Rock Levinson,[2] Peter J. Brophy,[3] Elior Peles,[4] and Steven S. Scherer[1]*

[1]Department of Neurology, The University of Pennsylvania Medical Center, Philadelphia
[2]University Colorado Health Science Center, C240 Physiology, Denver
[3]Department of Preclinical Veterinary Sciences, University of Edinburgh, Summerhall, Edinburgh, United Kingdom
[4]Department of Molecular Cell Biology, The Weizmann Institute of Science, Rehovot, Israel

We examined the organization of the molecular components of the nodal region in spontaneously diabetic BB-Wistar rats. Frozen sections and teased fibers from the sciatic nerves were immunostained for nodal (voltage-gated Na^+ channels, $ankyrin_G$, and ezrin), paranodal (contactin, Caspr, and neurofascin 155 kDa), and juxtaparanodal (Caspr2, the *Shaker*-type K^+ channels Kv1.1 and Kv1.2, and their associated subunit Kvβ2) proteins. All of these proteins were properly localized in myelinated fibers from rats that had been diabetic for 15–44 days, compared to age-matched, nondiabetic animals. These results demonstrate that the axonal membrane is not reorganized, so nodal reorganization is not likely to be the cause of nerve conduction slowing in this animal model of acute diabetes. J. Neurosci. Res. 65:139–149, 2001.

Key words: myelin; Schwann cells; neuropathy; sodium channels; potassium channels; Caspr; nodes

INTRODUCTION

The exquisite molecular architecture of myelinated fibers is the basis for saltatory conduction. Myelinated axons are completely covered by myelin sheaths, except at nodes of Ranvier, the small gaps (less than 1 μm in length) directly exposed to the extracellular milieu. By reducing the capacitance and/or increasing the resistance, myelin reduces current flow across the internodal axonal membrane, thereby facilitating saltatory conduction at nodes (Ritchie, 1995). The axonal membrane is organized in relation to the myelin sheath (Arroyo and Scherer, 2000; Peles and Salzer, 2000). The nodal axonal membrane is highly enriched in voltage-gated Na^+ channels, which are linked to the spectrin cytoskeleton by $ankyrin_G$ (Bennett et al., 1997; Berghs et al., 2000). The paranodal axonal membrane is enriched in contactin (Rios et al., 2000) and contactin-associated protein (Caspr; also known as paranodin), which together with the neurofascin 155 kDa (NF155) appear to form septate-like axoglial junctions (Einheber et al., 1997; Menegoz et al., 1997; Tait et al., 2000). The juxtaparanodal axonal membrane contains Caspr2, the *Shaker*-type potassium channels Kv1.1 and Kv1.2, and their associated β subunit, Kvβ2 (McNamara et al., 1993; Wang et al., 1993; Mi et al., 1995; Rhodes et al., 1996, 1997; Zhou et al., 1998; Rasband et al., 1998; Arroyo et al., 1999; Poliak et al., 1999; Vabnick et al., 1999). The distinct localization of these axonal proteins—into nodal, paranodal, and juxtaparanodal domains—provides compelling evidence that they are localized by *trans* interactions with myelinating glial cells, although the molecular basis of these interactions remains to be determined.

Although diabetes mellitus causes a number of clinically distinct neuropathies, the most common type is a length-dependent axonal neuropathy affecting sensory and motor fibers, usually referred to as diabetic neuropathy (Dyck and Thomas, 1999). In spite of an intensive effort, the mechanisms leading to axonal degeneration remain obscure, but metabolic and vascular changes are involved (Dyck and Thomas, 1999). Nerve conduction slowing is an early feature of human diabetic neuropathy. Nerve conduction slowing occurs in experimental animals, within 2 weeks of diabetes following alloxan (Eliasson, 1964) and streptozotocin (Greene et al., 1975) treatment and within 22 days after the onset of diabetes in BB-Wistar rats (Brismar and Sima, 1981; Sima and Hay, 1981). In BB-Wistar rats, this may be caused by an increased permeability to K^+ (P_K) of the axonal membrane, which occurs with 18 days of diabetes (Brismar and Sima, 1981). Because K^+ channels are normally found beneath the myelin sheath (Chiu and Ritchie, 1982), this altered P_K indicates either that K^+ channels are abnormally localized

*Correspondence to: Steven S. Scherer, MD, PhD, Department of Neurology, Room 460 Stemmler Hall, 36th Street and Hamilton Walk, The University of Pennsylvania Medical Center, Philadelphia, PA 19104. E-mail: sscherer@mail.med.upenn.edu

Received 25 February 2001; Revised 15 March 2001; Accepted 5 April 2001

in the nodal membrane or that the paranodal barrier is breached. The paranodal barrier is formed by a spiral of septate-like junctions (also known as transverse bands), which are sites of adhesion between the terminal loops of the myelin sheath and the paranodal axonal membrane (Hirano and Llena, 1995). The finding that diabetic nerves have altered axoglial junctions, so-called axoglial dysjunction (the term indicating the loss of the septate-like junctions/transverse bands; Sima and Brismar, 1985; Sima et al., 1986), favors the latter possibility.

Axoglial dysjunction, however, is not specific to diabetes; it has been noted in a variety of metabolic and inflammatory neuropathies, and its relevance to human diabetic neuropathy has been disputed (Giannini and Dyck, 1996; Thomas et al., 1996). Except for axoglial dysjunction, no other structural alterations have been found to account for the decrease in nerve conduction velocity and altered K^+ current in experimental diabetes. In that paranodal alternations are probably sufficient to slow nerve conduction velocity (Vabnick and Shrager, 1998), it is reasonable to suppose that, if diabetes alters the structure and/or function of the paranode, then this would also cause slowed conduction. In this study, we have reinvestigated this issue, taking advantage of recent advances in the understanding of the molecular architecture of myelinated fibers. The antibodies that have been developed against various molecular components of the nodal region allow a different approach to the question of whether diabetes alters the nodal architecture. Making comparisons to age-matched animals, we find no evidence that nodal (voltage-gated Na^+ channels, ankyrin$_G$, and ezrin), paranodal (contactin, Caspr, and NF155), or juxtaparanodal (Caspr2, Kv1.1, Kv1.2, and Kvβ2) proteins are reorganized in myelinated sciatic nerve fibers from BB-Wistar rats that have been diabetic for 15–44 days. These results demonstrate that the axonal membrane is not reorganized in this animal model of acute diabetes and call into question the idea that diabetes causes axoglial dysjunction.

MATERIALS AND METHODS

BBDP/Wor rats were purchased from Biomedical Research Models, Inc. (Worcester, MA). These rats were derived from the BB/Wistar rats and as of 1994 had been inbred for more than 48 generations (Guberski et al., 1993; Guberski, 1994). About 85% of these rats develop diabetes by 120 days of age, with an average onset at 70 days. The rats were raised at The University of Pennsylvania using the protocols of Dr. Ali Naji (Uchikoshi et al., 1999). Prior to the onset of diabetes, the rats were tested three times per week for glycosuria using urine test strips. Animals with urine glucose levels of 300 mg/dl or higher were tested within 2 hr for blood glucose concentration, using test strips on blood taken from the tail. Rats with a blood glucose concentration of 250 mg/dl or more were considered diabetic. Diabetic rats were given small daily doses of insulin (0.8–2.6 units) to maintain their health; this dose did not prevent hyperglycemia. The insulin dosage was determined according to the age, body weight, and presence of ketoacidosis and dehydration (Uchikoshi et al., 1999). The clinical history of the diabetic animals is summarized in Table I.

TABLE I. Health History of the Diabetic BB-Wistar Rats Used in This Study (Mean Daily Urine Glucose and Ketones)

Animal	Age at onset of diabetes (days)	Duration of diabetes (days)	Δ Weight after onset (gm)	Urine glucose (mean)[a]	Urine ketones (mean)[b]
1	74	15	−20	4	2.1
2	74	21	−65	4	2.4
3	76	21	+40	4	0
4	67	44	+51	4	1.5
5	58	44	+66	4	1.2

[a]0 = <150 mg/dl; 1 = 150–200; 2 = 200–250; 3 = 250–300; 4 = >300.
[b]0 = None detected; 1 = 5 mg/%; 2 = 15; 3 = 40; 4 = >80.

Rats were euthanized by CO_2 inhalation, and their sciatic nerves were removed. The nerves were placed in freshly prepared Zamboni's fixative (Zamboni and de Martino, 1967) for 30 min, then rinsed in 0.1 M phosphate buffer (PB; pH 7.4). Teased fibers were prepared from one nerve, dried on SuperFrost Plus glass slides, and stored at −20°C. Frozen sections (10 μm thick) were prepared from the other nerve as previously described (Scherer et al., 1995). The fibers and sections were permeabilized by immersion in −20°C acetone for 10 min, blocked at room temperature for at least 1 hr in 5% fish-skin gelatin containing 0.5% Triton ×-100 in PBS, and incubated for 24–48 hr at 4°C with various combinations of primary antibodies (Table II). For optimal labeling with the rabbit antiserum against NF155, the slides were dipped in Bouin's solution for 1 min, then rinsed in PB. After incubating with the primary antibodies, the slides were washed; incubated with the appropriate fluorescein-, rhodamine-, and cyanine 5-conjugated donkey anti-rabbit, anti-mouse, anti-rat, and/or anti-human cross-affinity-purified secondary antibodies (diluted 1:100; Jackson Immunoresearch Laboratories, West Grove, PA); and mounted with Vectashield (Vector Laboratories, Burlingame, CA). Specimens were examined by epifluorescence with TRITC, FITC, and Cy5 optics on a Leica DMR light microscope and photographed with a digital camera (Hamamatsu Orca) or with a Leica TCS laser scanning confocal microscope, followed by image manipulation with Adobe Photoshop and Canvas 7.

RESULTS

Organization of Nodal Proteins in Diabetic Nerves

We used spontaneously diabetic BB-Wistar rats, in which axoglial dysjunction has been the most thoroughly documented (Sima et al., 1986). We examined sciatic nerve fibers from five animals that had been diabetic for 15, 21, or 44 days (Table I); these times were selected because conduction slowing and axoglial dysjunction are well established in BB rats after 21 days and 44 days of diabetes, respectively (Sima and Hay, 1981; Sima and Brismar, 1985). Five age-matched non-prediabetic BB rats (the same strain) were used as controls, as well as nerves from young adult Sprague-Dawley rats. We analyzed frozen sections and teased fibers, but we favored the latter

TABLE II. Sources and Dilutions of Antibodies Used in This Study

Antibody	Dilution	Source/reference
Rabbit α mouse ezrin (90-3)	1:300	Amieva and Furthmayr, 1994, 1995
Rabbit α pan-Na^+ channels	1:500	Vabnick et al., 1997
Rabbit α $Na_v1.6$	1:100	Caldwell et al., 2000
Rabbit α $ankyrin_G$	1:100	Lambert et al., 1997
Rabbit α Caspr	1:1,000	Peles et al., 1999
Rabbit α NF155	1:750	Tait et al., 2000
Rabbit α contactin	1:500	Rios et al., 2000
Rabbit α Caspr2	1:50	Poliak et al., 1999
Rabbit α Kv1.1	1:200	Alomone Labs
Rabbit α Kv1.2	1:100	Alomone Labs
Mouse α pan-Na^+ channels	1:50	Sigma
Mouse α $ankyrin_G$	1:100	Zymed
Mouse α Caspr	1:50	Gift of Dr. James Trimmer
Mouse α Caspr	1:50	Poliak et al., 1999
Mouse α Kv1.1	1:50	Upstate Biotechnology
Mouse α Kv1.2	1:50	Upstate Biotechnology
Mouse α Kvβ2	1:50	Rhodes et al., 1996, 1997
Human IgG Fc/RPTPβ fusion	1:2	Peles et al., 1995
Rat α NFH (Ta51)	1:10	Lee et al., 1982, 1987

because they provide more structural details of the nodal region. To minimize the chance of spurious differences, specimens were processed and immunostained in parallel. We used many different antibodies (Table II), which, without exception, gave comparable results. Except for an occasional myelinated fiber undergoing Wallerian degeneration in 44 day diabetic nerves, we did not note any pathological changes in our material such as paranodal swelling or nodal widening.

Nodal Na^+ currents are reduced in myelinated fibers from acutely diabetic BB rats (Brismar and Sima, 1981; Brismar et al., 1987). We examined the localization of voltage-gated Na^+ channels with a rabbit antiserum and a monoclonal antibody against the same conserved sequence that is found in multiple members this family of channels (Goldin et al., 2000). As shown in Figures 1, 2, and 4, Na^+ channels were highly concentrated in nodal axonal membrane, with little paranodal, juxtaparanodal, or internodal staining, in both diabetic and nondiabetic nerves. We examined at least 50 small (fiber diameter 3 μm or less) and 50 large (fiber diameter 8 μm or more) teased fibers from every diabetic and age-matched BB animal, and we did not find a single example of Na^+ channel staining that extended beyond the nodal region. Similarly, in frozen sections of the sciatic nerve from these diabetic and age-matched BB animals, Na^+ channel staining was restricted to nodes (Fig. 4). We also examined the localization of $ankyrin_G$ with two different antibodies. In at least 50 small and 50 large myelinated fibers from every diabetic and age-matched BB animal, $ankyrin_G$ was restricted to the nodes and did not extend beyond the nodal region (data not shown). Fascicles of unmyelinated axons were uniformly stained with the pan-Na^+ channel antibodies (Fig. 4) and the $ankyrin_G$ antibodies (data not shown) in both diabetic and nondiabetic nerves.

The results described above demonstrate that the localization of nodal voltage-gated Na^+ channels and $ankyrin_G$ are unaffected by acute diabetes in BB rats. Because we used pan-Na^+ channel antibodies, however, we would not have been able to detect alterations in the types of nodal Na^+ channels. Caldwell and colleagues (2000) recently reported that $Na_v1.6$ is the main voltage-gated Na^+ channel in myelinated axons: All PNS nodes stain with an antiserum against $Na_v1.6$. To determine whether $Na_v1.6$ was the predominant voltage-gated Na^+ channel in diabetic nerves, we examined more than 50 small (fiber diameter 3 μm or less) and 50 large (fiber diameter 8 μm or more) fibers. Every node was stained, and no myelinated fibers had $Na_v1.6$ staining that extended beyond the nodal region (Fig. 1E, E′).

Cell adhesion molecules on microvilli have been postulated to localize Na^+ channels to nodes (Bennett et al., 1997; Scherer et al., 2001). We have recently found that all three members of the ezrin, radixin, and moesin (ERM) family of proteins, are expressed in the nodal microvilli of myelinating Schwann cells (Scherer et al., 2001). To determine whether the nodal microvilli are disrupted in acutely diabetic nerves, we immunostained teased fibers with a rabbit antiserum against ezrin (Fig. 1 D, D′). Examining at least 50 large and 50 small myelinated fibers from every diabetic nerve and nondiabetic nerve, we did not find any examples of altered ezrin staining at nodes.

Organization of Paranodal Proteins in Diabetic Nerves

We examined the localization of Caspr, which is highly enriched in the paranodal axonal membrane (Einheber et al., 1997; Menegoz et al., 1997). In both teased fibers (Figs. 1, 3, 5) and frozen sections (data not shown), paranodes had prominent Caspr immunoreactivity. In at least 50 large and 50 small teased myelinated fibers from every diabetic nerve and nondiabetic nerve, we did not find any examples of altered patterns of Caspr staining. As in normal nerves (Arroyo et al., 1999), the Caspr antibodies inconsistently stained an internodal strand that apposes the inner mesaxon (termed *juxtamesaxonal* staining; Peles and Salzer, 2000) and a ring of internodal staining that apposes the inner aspect of incisures (*juxtaincisural* staining).

Caspr was originally discovered owing to its *cis* interaction with contactin (Peles et al., 1997), and Rios et al. (2000) have recently shown that paranodes have contactin immunoreactivity. In other tissues, contactin has *trans* interactions with receptor protein tyrosine phosphatase-β (RPTPβ; Peles et al., 1995), but RPTPβ has not been detected in myelinated fibers (Rios et al., 2000). To determine whether acute diabetes alters the distribution of contactin, we labeled teased fibers from all of our diabetic and nondiabetic/control nerves. Examining at least 50

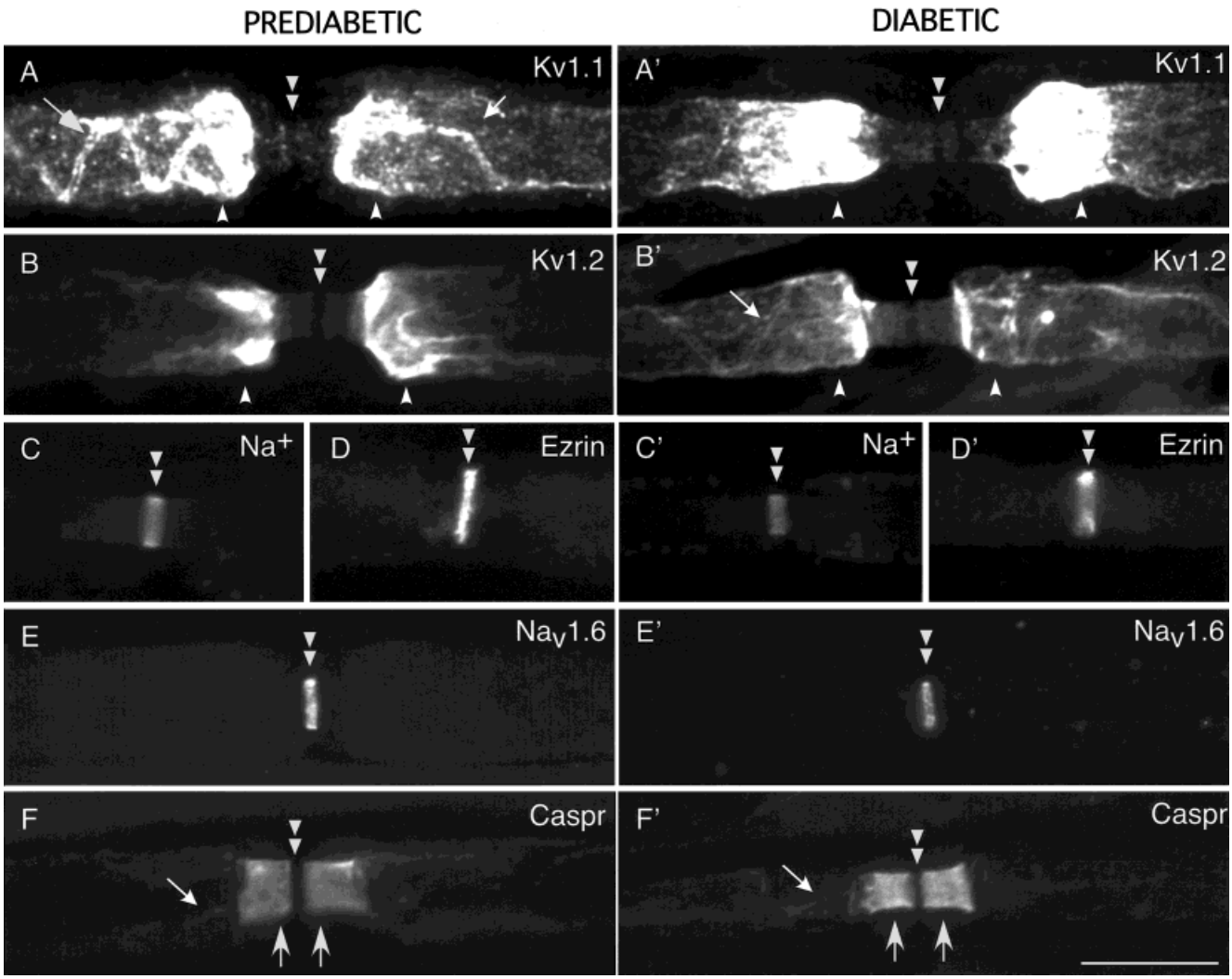

Fig. 1. Diabetic myelinated fibers have a normal molecular architecture. Photomicrographs of myelinated fibers from teased sciatic nerves; in each pair of photomicrographs, the prediabetic animal was the same age as the diabetic animal. The fibers were immunostained with a rabbit antiserum against Kv1.1 (**A,A′;** 44 days diabetic), a rabbit antiserum against Kv1.2 (**B,B′;** 21 days diabetic), a mouse pan-Na^+ channel monoclonal antibody (**C,C′;** 21 days diabetic), a rabbit antiserum against ezrin (**D,D′;** 44 days diabetic), a rabbit antiserum against $Na_v1.6$ (**E,E′;** 44 days diabetic), and a rabbit antiserum against Caspr (**F,F′;** 21 days diabetic). Double arrowheads indicate nodes, large arrows indicate paranodes, small arrows indicate "juxtamesaxonal" staining, and single arrowheads indicate juxtaparanodes. The images of Kv1.1 and Kv1.2 staining were overexposed to show the lower level of paranodal staining and the gap of nodal staining. Scale bar = 10 μm.

large and 50 small myelinated fibers from every diabetic nerve and nondiabetic nerve, we did not find any examples of altered patterns of contactin staining using either a rabbit antiserum against contactin (Fig. 5) or a human IgG Fc/RPTPβ fusion protein that binds contactin (data not shown).

Although the Caspr/contactin complex is thought to participate in the formation of the septate-like junctions that are found at paranodes (Arroyo and Scherer, 2000; Peles and Salzer, 2000) the *trans*-interacting protein(s) on the paranodal loops of myelinating cells remains to be established. Recently Tait and colleagues (2000) have shown that NF155 is localized to septate-like junctions, although they did not find direct binding to Caspr. We labeled teased fibers with a rabbit antiserum against NF155 and found that that it localized to the paranodal region as well as incisures and inner mesaxon of myelinating Schwann cells (Fig. 5). Examining at least 50 large and 50 small myelinated fibers from every diabetic nerve and nondiabetic nerve, we did not find any examples of altered patterns of NF155 staining.

Organization of Juxtaparanodal Proteins in Diabetic Nerves

The localizations of Kv1.1 and Kv1.2 were similarly examined in teased fibers from diabetic and nondiabetic nerves. As shown in Figures 1–4, there was prominent jux-

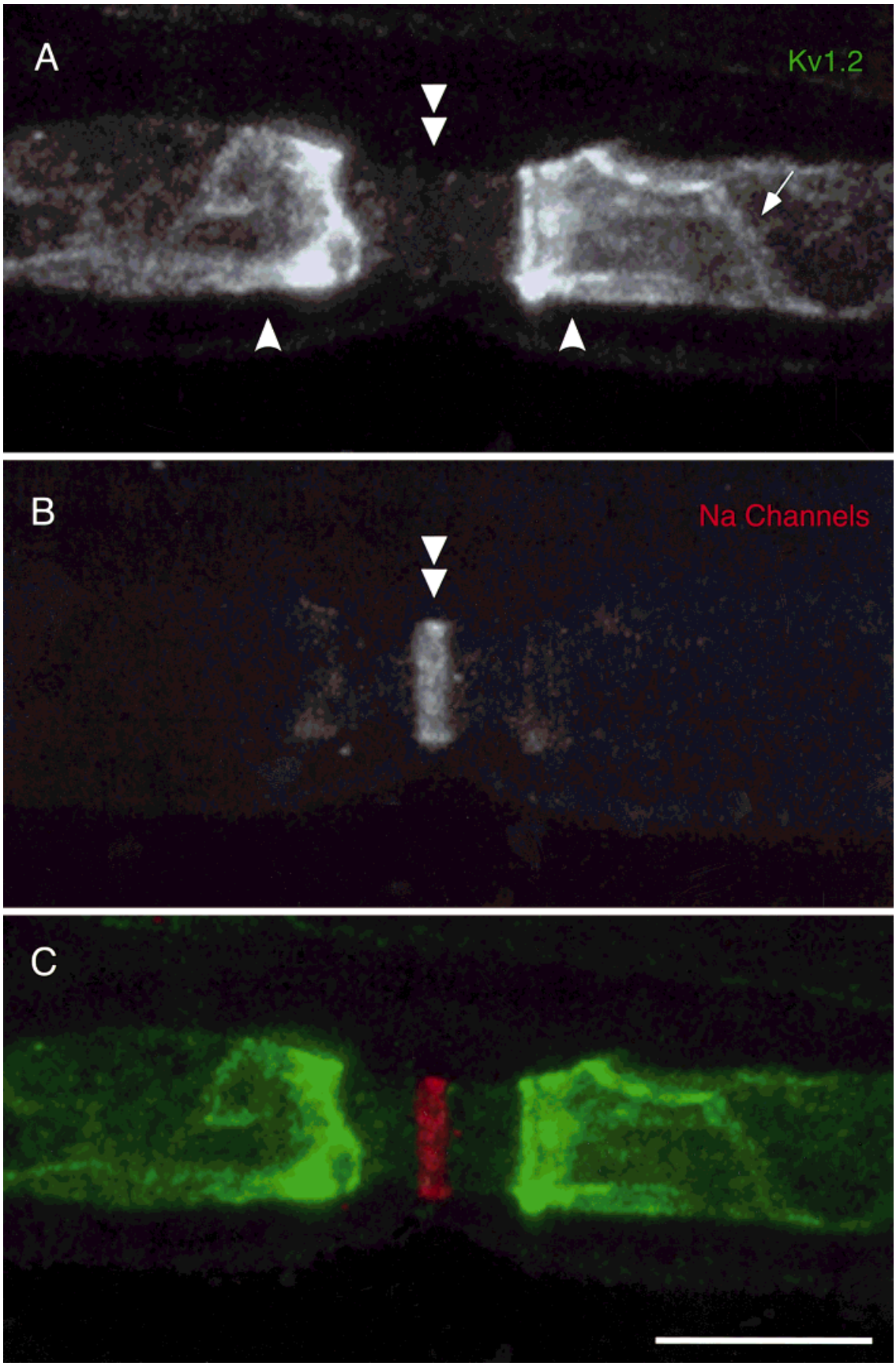

Fig. 2. Voltage-gated Na^+ channels and *Shaker*-type K^+ channels are properly localized in teased myelinated fibers from diabetic animals. Confocal micrographs of a single, teased fiber from a diabetic animal (21 days diabetic). The fiber was immunostained with a rabbit antiserum against Kv1.2 (**A**) and a mouse pan-Na^+ channel monoclonal antibody (**B**); **C** shows the merged image. Symbols as in Figure 1. The image of Kv1.2 staining was slightly overexposed to show the lower level of paranodal and nodal staining; this fiber does not have a well-defined gap in nodal Kv1.2 staining. Scale bar = 10 μm.

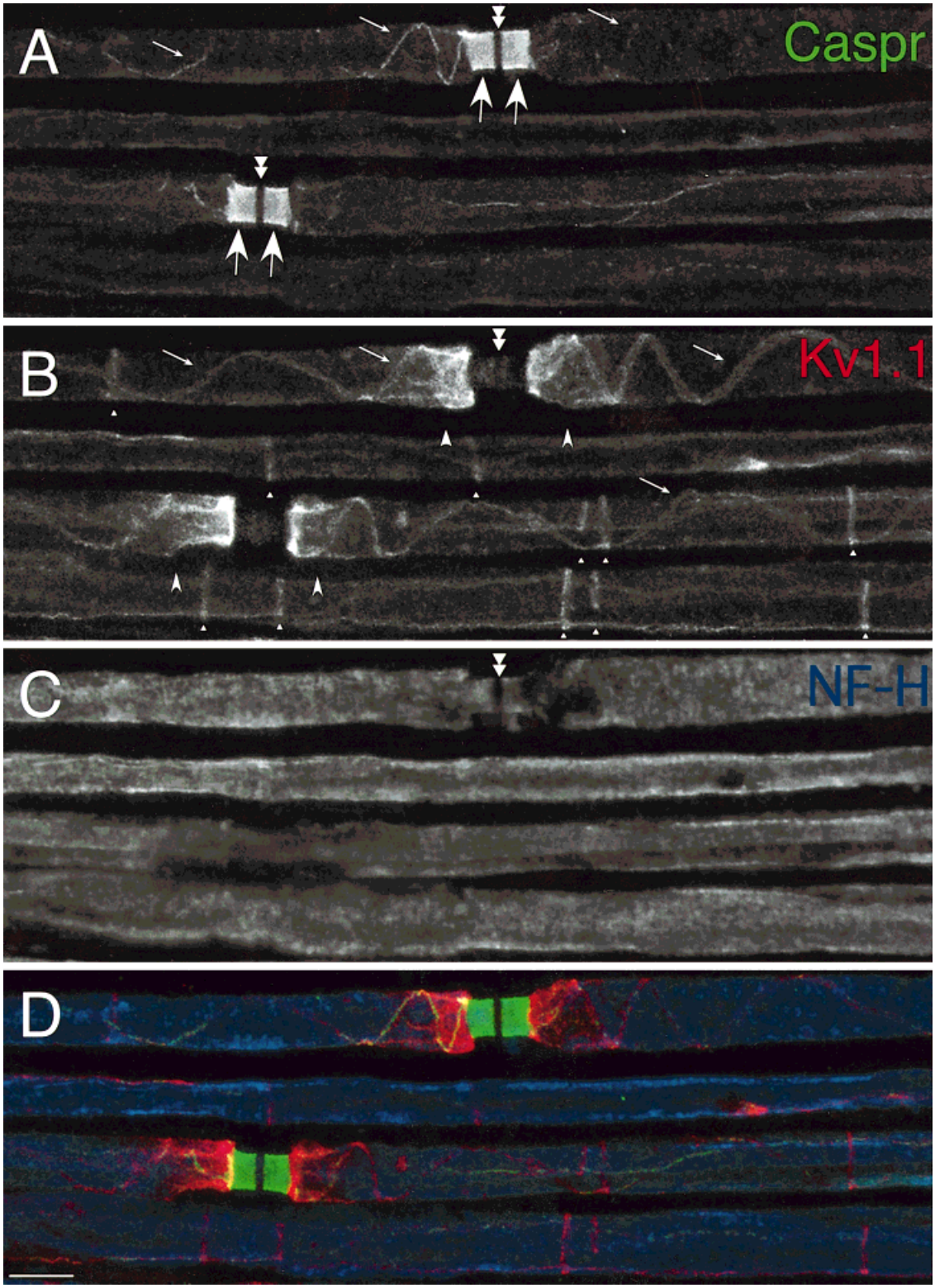

Fig. 3. Paranodal, juxtaparanodal, and internodal distribution of Caspr and Kv1.1 are properly localized in diabetic myelinated fibers. Confocal micrographs of teased fibers from a diabetic animal (21 days diabetic). The fibers were immunostained with a rabbit antiserum against Caspr (**A**), a mouse monoclonal antibody against Kv1.1 (**B**), and a rat monoclonal antibody against NFH (**C**); **D** shows the merged images. Symbols as in Figure 1. Scale bar = 10 μm.

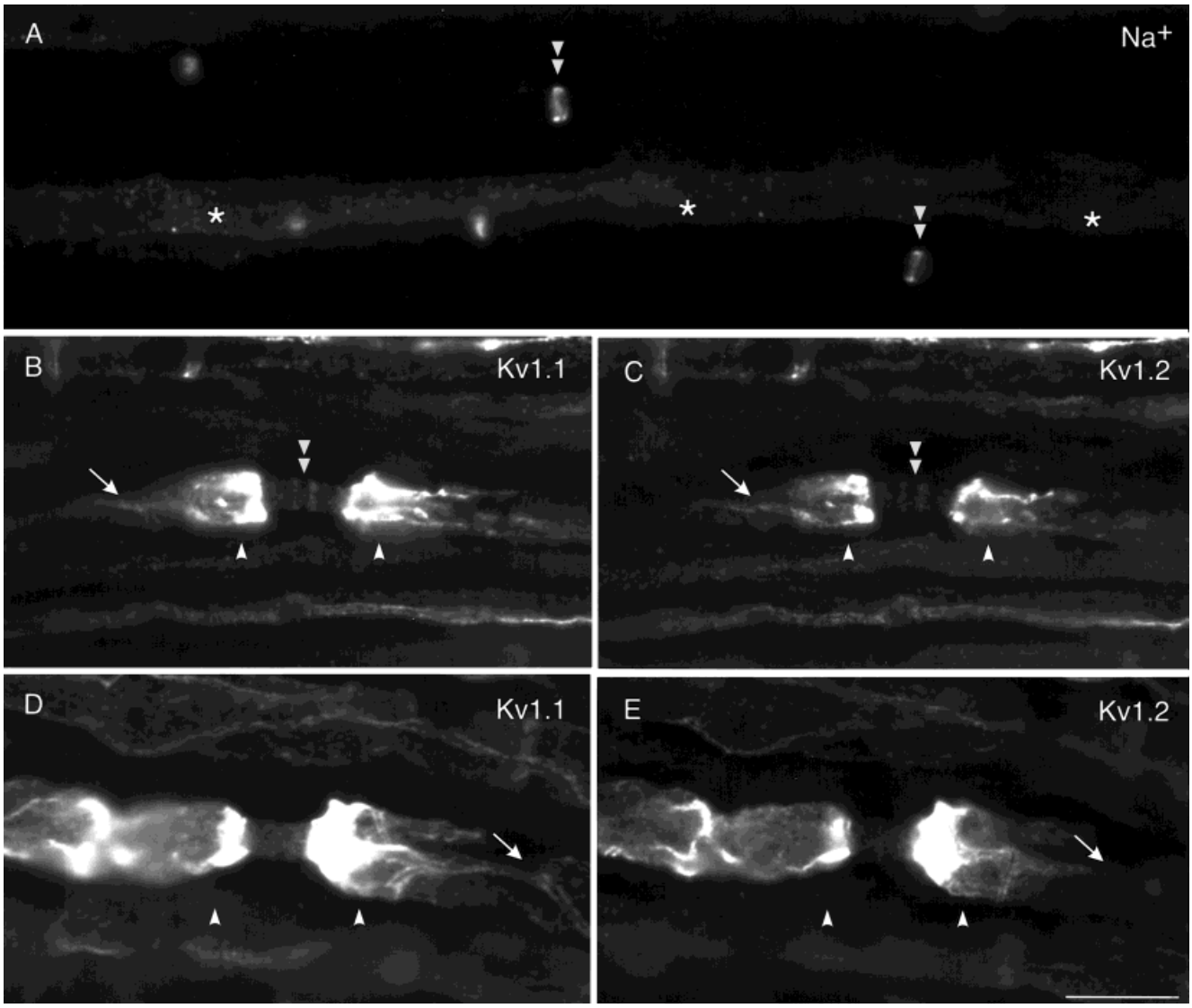

Fig. 4. Voltage-gated Na^+ channels and *Shaker*-type K^+ channels are properly localized in myelinated fibers from diabetic animals. Photomicrographs of myelinated fibers from frozen sections of diabetic sciatic nerves, stained with a mouse pan-Na^+ channel monoclonal antibody (**A**), a rabbit antiserum to Kv1.1 (**B**) or Kv1.2 (**E**), or a mouse monoclonal antibody to Kv1.2 (**C**) or Kv1.2 (**D**). Symbols as in Figure 1. The images of Kv1.1 and Kv1.2 staining (B–E) were overexposed to show the lower level of paranodal staining and the presence or absence of nodal staining. The fiber in B and C has a well-defined gap in K^+ channel staining, whereas the one shown in D and E does not. The asterisks in A indicate Na^+ channel staining of a fascicle of unmyelinated axons. Scale bar = 10 μm.

taparanodal staining and a lower level of paranodal staining in control/nondiabetic nerves with Caspr2. Examining at least 50 large and 50 small myelinated fibers from every diabetic nerve, we did not find any examples of altered Kv1.1 or Kv1.2 staining. In addition, just as in nondiabetic nerves, most myelinated fibers in diabetic nerves had juxtamesaxonal as well as juxtaincisural Kv1.1 and Kv1.2 staining. The juxtamesaxonal as well as juxtaincisural staining could often be resolved into a pair of lines (Figs. 1–4) that flank a single line of Caspr (Fig. 3) or contactin (data not shown) staining (Arroyo et al., 1999; Rios et al., 2000).

To determine whether Kv1.1 and Kv1.2 are colocalized in diabetic nerves as they are in normal nerves, we labeled teased fibers and sections with either a rabbit antiserum to Kv1.1 and a monoclonal antibody to Kv1.2 or a rabbit antiserum to Kv1.2 and a monoclonal antibody to Kv1.1. We have previously shown that the antibodies against Kv1.1 and Kv1.2 do not stain myelinated axons in Kv1.1- and Kv.1.2-null mice, respectively, demonstrating their specificity (Arroyo et al., 1999). As shown in Figure 4B–E, both combinations of antibodies labeled the same structures. Thus, neither the distribution nor the colocalization of Kv1.1 or Kv1.2 of myelinated fibers was altered by acute diabetes.

Electrophysiological studies indicate that mammalian nodes lack K^+ channels (Chiu et al., 1999) whereas Brismar and colleagues (Brismar, 1980, 1983; Brismar and

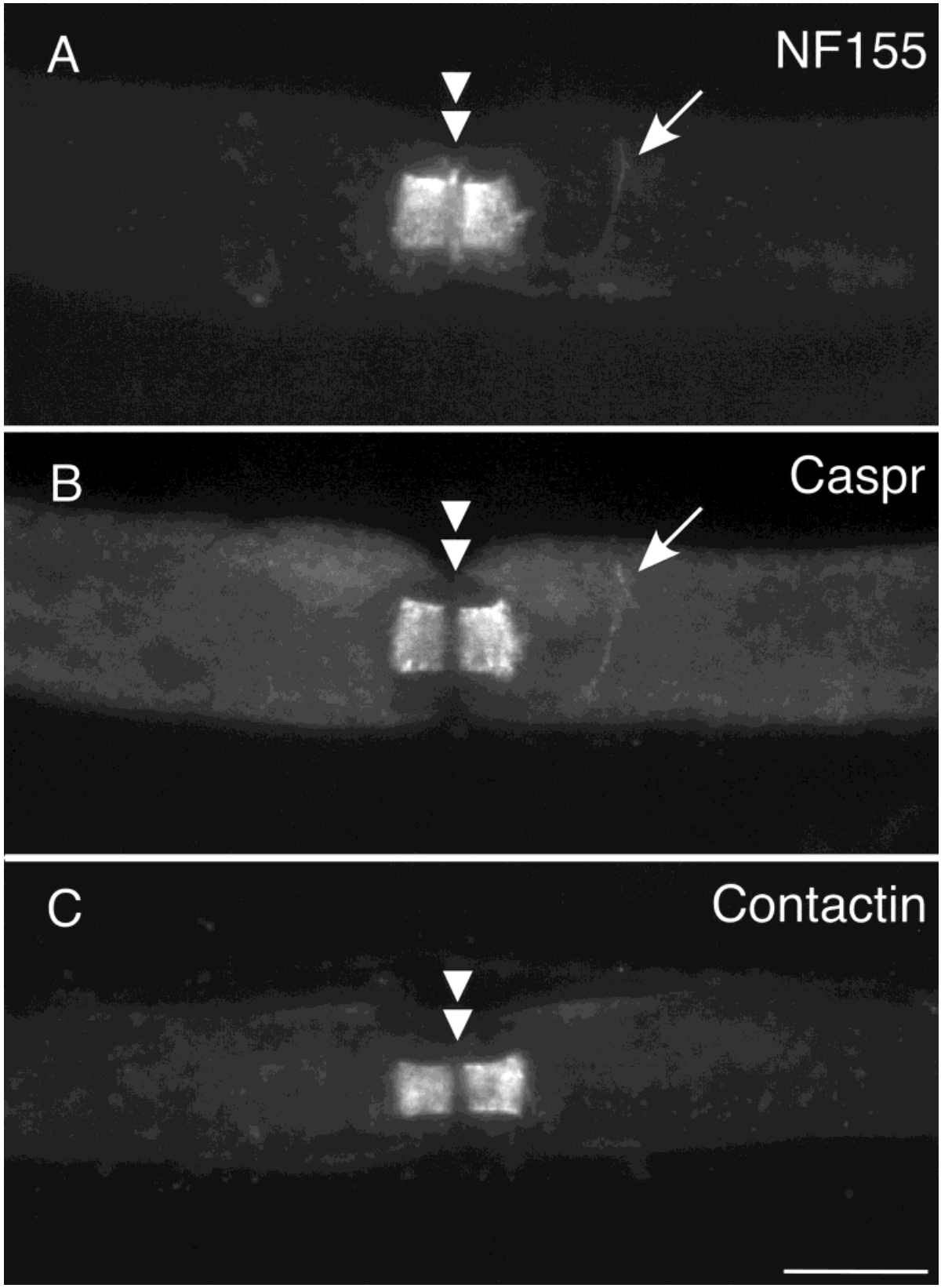

Fig. 5. Paranodal markers are properly localized in myelinated fibers from diabetic animals. Photomicrographs of teased myelinated fibers from a diabetic animal (21 days diabetic). Symbols as in Figure 1. **A** and **B** show a fiber that has been doubly labeled with a rabbit antiserum against NF155 and a monoclonal antibody against Caspr. At the paranode and internode, NF155 and Caspr are colocalized, but there appears to be a disk of NF155 staining in the Schwann cell microvilli. In **C,** a rabbit antiserum against contactin labels the paranodal region of a myelinated fiber. Scale bar = 10 μm.

Sima, 1981) found nodal K^+ channels in diabetic nerves. Thus, we were particularly interested in determining whether the nodal membrane of myelinated fibers from diabetic nerves had Kv1.1 or Kv1.2 staining. This analysis proved to be impractical; it was not possible to visualize reliably the thin gap of absent Kv1.1 or Kv1.2 staining even in nerves from nondiabetic BB or Sprague-Dawley rats, much less in myelinated fibers from diabetic BB rats. We examined both teased fibers and frozen sections in this regard; examples of nodes with and without gaps of Kv1.1 and Kv1.2 staining are shown in Figures 1–4. No differences in the extent of nodal staining with antibodies against Kv1.1 vs. those against Kv1.2 were detected, although the rabbit antisera stained more robustly than did the mouse monoclonal antibodies.

We also examined the localization of Kvβ2 and Caspr2 in diabetic and control BB nerves. There was little Kvβ2 immunoreactivity in our samples, as was expected because they were fixed (Arroyo et al., 1999). Both diabetic and control BB nerves had juxtaparanodal Caspr2 staining (data not shown).

DISCUSSION

We analyzed the localization of several proteins that are localized to nodal, paranodal, and juxtaparanodal region in acutely diabetic BB-Wistar rats, a well-studied animal model of acute diabetes (Mendell et al., 1981; Sima and Hay, 1981; Sima et al., 1986, 2000; Brismar et al., 1987; Guberski et al., 1993; Guberski, 1994). We find no evidence that acute diabetes affects the localization of nodal (voltage-gated Na^+ channels, ankyrin$_G$, and ezrin), paranodal (contactin, Caspr, and NF155), or juxtaparanodal (Caspr2, Kv1.1, Kv1.2, and Kvβ2) proteins. These results are inconsistent with the idea that acute diabetes alters the structure of the paranode or reorganizes the axonal membrane. This conclusion rests on the examination of thousands of myelinated fibers, using multiple antibodies, from animals that had had diabetes for an appropriate period of time (15–44 days).

Axoglial Dysjunction in Diabetic Neuropathy

The paranode is a uniquely specialized region of myelinated fibers. Where the lateral edge of the myelin sheath spirals around the axon, the glial loops form axoglial junctions with the underlying axonal membrane (Arroyo and Scherer, 2000; Peles and Salzer, 2000). In both the PNS and the CNS, the glial loops appear to be connected to the axolemma by a series of electron-dense knobs, the septate-like junctions/transverse bands. Septate-like junctions contain contactin, Caspr, NF155, and perhaps other molecules. Unlike the septate junctions of insects, which form a "tight" barrier, septate-like junctions form a leaky barrier to the diffusion of extracellular molecules, excluding the entry of large (horseradish peroxidase; 40,000 kDa), but not small (microperoxidase; 1,900 kDa), proteins into the periaxonal space (Feder, 1971; Towfighi and Gonatas, 1977). Septate-like junctions also appear to alter the localization of intrinsic membrane proteins of axons; as in *cgt*-null and *contactin*-null mice, Kv1.1 and Kv1.2 channels are found in the paranodal region (Dupree et al., 1999; Berglund et al., 2000).

Sima and colleagues reported the loss of septate-like junctions/transverse bands at axoglial junctions, which they termed axoglial dysjunction. This was first noted in the spontaneously diabetic BB rat (Sima et al., 1986) and subsequently in nerves from diabetic humans (Sima et al., 1988, 1993). In BB rats, insulin treatment only partially restored motor nerve conduction velocity and did not restore the loss of transverse bands (Sima and Brismar, 1985; Sima et al., 1986). In humans treated with the aldose reductase inhibitor sorbinil, however, an improvement in nerve conduction velocity correlated with restoration of the transverse bands (Sima et al., 1993). Axoglial dysjunction, however, is not specific to diabetes; it has been noted in a variety of metabolic and inflammatory neuropathies; and whether axoglial dysjunction is even a hallmark of human and diabetic neuropathy is disputed (Giannini and Dyck, 1996; Thomas et al., 1996). Moreover, a previous freeze-fracture study on diabetic nerve found little evidence for axoglial dysjunction, but the authors used a spontaneously diabetic line of mice (*db/db*) in which axoglial dysjunction has not been reported (Shirasaki and Rosenbluth, 1991).

We reinvestigated the issue of whether acute diabetes causes axoglial dysjunction in diabetic BB rats, in which this phenomenon was originally reported (Sima and Brismar, 1985; Sima et al., 1986). We reasoned that, if axoglial dysjunction occurs, then it should disrupt the organization of paranodal and juxtaparanodal proteins, perhaps in a manner similar to what has been described for *cgt*- and *contactin*-null mice. In *cgt*-null mice, septate-like junctions are absent or disorganized (Bosio et al., 1998; Dupree et al., 1998), and contactin, Caspr, and NF155 are not localized to paranodes (Dupree et al., 1999; Peles, personal observations). Similarly, in *contactin*-null mice, septate-like junctions are absent, and Caspr is not localized to paranodes (Berglund et al., 2000). Furthermore, in both *cgt*- and *contactin*-null mice, the highest accumulations of Kv1.1 and Kv1.2 are found in the paranode, not the juxtaparanode (Dupree et al., 1999; Berglund et al., 2000). In addition, nerve conduction velocities are markedly slowed and were abnormally affected by K^+ channel blockers in these mice (Bosio et al., 1996; Coetzee et al., 1996; Berglund et al., 2000). Thus, when septate-like junctions are missing, there is a clear concordance between the ultrastructural findings and the localization of paranodal and juxtaparanodal proteins. It seems highly unlikely, therefore, that we could have missed anything but a subtle derangement of septate-like junctions in our diabetic rats.

Other Changes in Diabetic Neuropathy

Although axoglial dysjunction is controversial, it is well established that nerve conduction velocity slows during acute diabetes in both rodents and humans (Dyck and Thomas, 1999). Furthermore, at least some of this slowing is reversible with treatment with insulin, myoinositol, or aldose reductase inhibitors (Greene et al., 1975; Mayer and Tomlinson, 1983) and other agents (Dyck and Thomas,

1999). In that paranodal alternations are probably sufficient to slow nerve conduction (Vabnick and Shrager, 1998), paranodal changes could also account for the dramatic increases in nodal P_K in diabetic rats (Brismar, 1980; Brismar and Sima, 1981). Either insertion of K^+ channels into the nodal membrane or "loosening" of axoglial junctions could expose paranodal and/or juxtaparanodal Kv1.1 and 1.2 channels and could lead to slowing of axonal conduction. Although we attempted to investigate this issue, the apparent presence of Kv1.1 and Kv1.2 channels in the nodal membrane of many axons, even in nondiabetic rats, precluded such an analysis with our material.

Paranodal swellings of large myelinated fibers from diabetic BB rats were reported in one study (Sima and Brismar, 1985) but not in another (Mendell et al., 1981). It is conceivable that we missed this feature, in that we usually labeled molecules that are not part of the myelin sheath. For the same reason, however, if acute diabetes causes paranodal swelling, it is unlikely to affect axons. In agreement with Sima and Brismar (1985), we did not find widened nodes in diabetic nerves, but we did not find altered patterns of voltage-dependent Na^+ channels in diabetic nerves, as reported by Cherian et al. (1996). Their published examples show Na^+ channel staining that extends well into the paranodes, even in normal animals, indicating that there are fundamental technical problems with their methodology. In this regard, a serious problem with the antiserum they used has recently been raised (Ritchie et al., 2000). In view of these technical issues, and in light of our data to the contrary, the report of altered Na^+ channel staining in diabetic BB rats (Cherian et al., 1996) should be viewed with skepticism.

ACKNOWLEDGMENTS

This work was supported by a grant from the Juvenile Diabetes Foundation to S.S.S.; E.J.A. was supported by a grant from the Charcot-Marie-Tooth Association. We thank Drs. Heinz Furthmayr, Stephen Lambert, Virginia Lee, and James Trimmer for their generous gifts of antibodies; Dr. Mark Brown for his comments on the manuscript; and Dr. Ali Naji for the BB-Wistar rats.

REFERENCES

Arroyo EJ, Scherer SS. 2000. On the molecular architecture of myelinated fibers. Histochem Cell Biol 113:1–18.

Arroyo EJ, Xu Y-T, Zhou L, Messing A, Peles E, Chiu SY, Scherer SS. 1999. Myelinating Schwann cells determine the internodal localization of Kv1.1, Kv1.2, Kvβ2, and Caspr. J Neurocytol 28:333–347.

Bennett V, Lambert S, Davis JQ, Zhang X. 1997. Molecular architecture of the specialized axonal membrane at the node of Ranvier. Soc Gen Physiol 52:107–120.

Berghs S, Aggujaro D, Dirkx R, Maksimova E, Stabach P, Hermel JM, Zhang JP, Philbrick W, Slepnev V, Ort T, Solimena M. 2000. beta IV spectrin, a new spectrin localized at axon initial segments and nodes of Ranvier in the central and peripheral nervous system. J Cell Biol 151: 985–1001.

Berglund EO, Boyle MET, Murai KK, Peles E, Weber L, Ranscht B. 2000. Contactin regulates axon-Schwann cell interactions at the paranode in myelinated peripheral nerve. Soc Neurosci Abstr 26:1081.

Bosio A, Binczek E, Stoffel W. 1996. Functional breakdown of the lipid bilayer of the myelin membrane in central and peripheral nervous system myelin by disrupted galactocerebroside synthesis. Proc Natl Acad Sci USA 93:13280–13285.

Bosio A, Bussow H, Adam J, Stoffel W. 1998. Galactosphingolipids and axon–glial interaction in myelin of the central nervous system. Cell Tissue Res 292:199–210.

Brismar T. 1980. Potential clamp experiments on myelinated nerve fibres from alloxan diabetic rats. Acta Physiol Scand 105:384–386.

Brismar T. 1983. Nodal function of pathological nerve fibers. Experienta 39:946–953.

Brismar T, Sima AAF. 1981. Changes in nodal function in nerve fibers of the spontaneously diabetic BB-Wistar rat: potential clamp analysis. Acta Physiol Scand 113:499–506.

Brismar T, Sima AAF, Greene DA. 1987. Reversible and irreversible nodal dysfunction in diabetic neuropathy. Ann Neurol 21:504–507.

Caldwell JH, Schaller KL, Lasher RS, Peles E, Levinson SR. 2000. Sodium channel $Na_V1.6$ is localized at nodes of Ranvier, dendrites, and synapses. Proc Nat Acad Sci USA 97:5616–5620.

Cherian PV, Kamijo M, Angelides KJ, Sima AAF. 1996. Nodal Na^+-channel displacement is associated with nerve-conduction slowing in the chronically diabetic BB/W rat: prevention by aldose reductase inhibition. J Diabetes Complic 10:192–200.

Chiu SY, Ritchie JM. 1982. Evidence for the presence of potassium channels in the internode of frog myelinated nerve fibres. J Physiol 322:485–501.

Chiu SY, Zhou L, Zhang C-L, Messing A. 1999. Analysis of potassium channel functions in mammalian axons by gene knockouts. J Neurocytol 28:349–364.

Coetzee T, Fujita N, Dupree J, Shi R, Blight A, Suzuki K, Suzuki K, Popko B. 1996. Myelination in the absence of galactocerebroside and sulfatide: normal structure with abnormal function and regional instability. Cell 86:209–219.

Dupree JL, Coetzee T, Blight A, Suzuki K, Popko B. 1998. Myelin galactolipids are essential for proper node of Ranvier formation in the CNS. J Neurosci 18:1642–1649.

Dupree JL, Girault JA, Popko B. 1999. Axo–glial interactions regulate the localization of axonal paranodal proteins. J Cell Biol 147:1145–1151.

Dyck PJ, Thomas PK. 1999. Diabetic neuropathy. Philadelphia: W. B. Saunders. 560 p.

Einheber S, Zanazzi G, Ching W, Scherer SS, Milner TA, Peles E, Salzer JL. 1997. The axonal membrane protein Caspr/Neurexin IV is a component of the septate-like paranodal junctions that assemble during myelination. J Cell Biol 139:1495–1506.

Eliasson SG. 1964. Nerve conduction changes in experimental diabetes. J Clin Invest 43:2353–2358.

Feder N. 1971. Microperoxidase—an ultrastructural tracer of low molecular weight. J Cell Biol 51:339–343.

Giannini C, Dyck PJ. 1996. Axoglial dysjunction: a critical appraisal of definition, techniques, and previous results. Microsc Res Techn 34:436–444.

Goldin AL, Barchi RL, Caldwell JH, Hofmann F, Howe JR, Hunter JC, Kallen RG, Mandel G, Meisler MH, Netter YB, Noda M, Tamkun MM, Waxman SG, Wood JN, Catterall WA. 2000. Nomenclature of voltage-gated sodium channels. Neuron 28:365–368.

Greene DA, De Jesus PV, Winegrad AI. 1975. Effects of insulin and dietary myoinositol on impaired peripheral motor nerve conduction velocity in acute streptozotocin diabetes. J Clin Invest 55:1326–1336.

Guberski DL. 1994. Diabetes-prone and diabetes-resistant BB rats: animals models of spontaneous and virally induced diabetes mellitus, lymphocytic thyroiditis, and collagen-induced arthritis. ILAR News, Vol 35.

Guberski DL, Butler L, Manzi SM, Like AA. 1993. The BBZ/Wor rat: clinical characteristics of the diabetic syndrome. Diabetologia 36:912–919.

Hirano A, Llena JF. 1995. Morphology of central nervous system axons. In: Waxman SG, Kocsis JD, Stys PK, editors. The axon. New York: Oxford University Press. p 49–67.

Lambert S, Davis JQ, Bennett V. 1997. Morphogenesis of the node of Ranvier: co-clusters of ankyrin and ankyrin-binding integral proteins define early developmental intermediates. J Neurosci 17:7025–7036.

Mayer JH, Tomlinson DR. 1983. Prevention of defects of axonal transport and nerve conduction velocity by oral administration of myo-inositol or an aldose reductase inhibitor in streptozotocin-diabetic rats. Diabetologia 25:433–438.

McNamara NMC, Muniz ZM, Wilkin GP, Dolly JO. 1993. Prominent location of a K^+ channel containing the a subunit Kv1.2 in the basket cell nerve terminals of rat cerebellum. Neuroscience 57:1039–1045.

Mendell JR, Sahenk Z, Warmolts JR, Marshall JK, Thibert P. 1981. The spontaneously diabetic BB rat. Morphological and physiological studies of peripheral nerve. J Neurol Sci 52:103–115.

Menegoz M, Gaspar P, Le Bert M, Galvez T, Burgaya F, Palfrey C, Ezan P, Arnos F, Girault J-A. 1997. Paranodin, a glycoprotein of neuronal paranodal membranes. Neuron 19:319–331.

Mi HY, Deerinck TJ, Ellisman MH, Schwarz TL. 1995. Differential distribution of closely related potassium channels in rat Schwann cells. J Neurosci 15:3761–3774.

Peles E, Salzer JL. 2000. Molecular domains of myelinated fibers. Curr Opin Neurobiol 10:558–565.

Peles E, Nativ M, Campbell PL, Sakurai T, Martinez R, Lev S, Clary DO, Schilling J, Barnea G, Plowman GD, Grumet M, Schlessinger J. 1995. The carbonic anhydrase domain of receptor tyrosine phosphatase β is a functional ligand for the axonal cell recognition molecule contactin. Cell 82:251–260.

Peles E, Nativ M, Lustig M, Grumet M, Martinez R, Plowman GD, Schlessinger J. 1997. Identification of a novel contactin-associated transmembrane receptor with multiple domains implicated in protein-protein interactions. EMBO J 16:978–988.

Poliak S, Gollan L, Martinez R, Custer A, Einheber S, Salzer JL, Trimmer J, Shrager P, Peles E. 1999. Caspr2, a new member of the neurexin superfamily is localized at the juxtaparanodes of myelinated axons and associates with K^+ channels. Neuron 24:1037–1047.

Rasband M, Trimmer JS, Schwarz TL, Levinson SR, Ellisman MH, Schachner M, Shrager P. 1998. Potassium channel distribution, clustering, and function in remyelinating rat axons. J Neurosci 18:36–47.

Rhodes KJ, Monaghan MM, Barrezueta NX, Nawoschik S, Bekelearcuri Z, Matos MF, Nakahira K, Schechter LE, Trimmer JS. 1996. Voltage-gated K^+ channel beta subunits: expression and distribution of Kvβ1 and Kvβ2 in adult rat brain. J Neurosci 16:4846–4860.

Rhodes KJ, Strassle BW, Monaghan MM, Bekele-Arcuri Z, Matos MF, Trimmer JS. 1997. Association and colocalization of the Kvβ1 and Kvβ2 in with Kv1 α-subunits in mammalian brain K^+ channel complexes. J Neurosci 17:8646–8258.

Rios JC, Melandez Vasquez CV, Einheber S, Lustig M, Grumet M, Hemperly J, Peles E, Salzer JL. 2000. Contactin-associated protein (Caspr) and contactin form a complex that is targeted to the paranodal junctions during myelination. J Neurosci 20:8354–8364.

Ritchie JM. 1995. Physiology of axons. In: Waxman SG, Kocsis JD, Stys PK, editors. The axon. New York: Oxford University Press. p. 68–96.

Ritchie JM, Black JA, Waxman SG. 2000. Sodium channels in the cytoplasm of Schwann cells (retraction). Proc Natl Acad Sci USA 97:1949.

Scherer SS, Deschênes SM, Xu Y-T, Grinspan JB, Fischbeck KH, Paul DL. 1995. Connexin32 is a myelin-related protein in the PNS and CNS. J Neurosci 15:8281–8294.

Scherer SS, Xu T, Crino P, Arroyo EJ, Gutmann DH. 2001. Ezrin, radixin, and moesin are components of Schwann cell microvilli. J Neurosci Res (this issue).

Shirasaki N, Rosenbluth J. 1991. Structural abnormalities in freeze-fractured sciatic nerve fibres of diabetic mice. J Neurocytol 20:573–584.

Sima AF, Brismar T. 1985. Reversible diabetic nerve dysfunction: structural correlates to electrophysiological abnormalities. Ann Neurol 18:21029.

Sima AAF, Hay K. 1981. Functional considerations and pathogenetic considerations of the neuropathy in the spontaneously diabetic BB-Wistar rat. Neuropathol Appl Neurobiol 7:341–350.

Sima AF, Lattimer SA, Yagihashi S, Greene DA. 1986. Axo–glial dysjunction. A novel structural lesion that accounts for poorly reversible slowing of nerve conduction in the spontaneously diabetic bio-breeding rat. J Clin Invest 77:474–484.

Sima AF, Nathaniel V, Bril V, McEwen TAJ, Greene DA. 1988. Histopathological heterogeneity of neuropathy in insulin-dependent and non-insulin-dependent diabetes, and demonstration of axo-glial dysjunction in human diabetic neuropathy. J Clin Invest 81:349–364.

Sima AF, Prashar A, Nathaniel V, Bril V, Werb MR, Greene DA. 1993. Overt diabetic neuropathy: repair of axo-glial dysjunction and axonal atrophy by aldose reductase inhibition and its correlation to improvement in nerve conduction. Diabetic Med 10:115–121.

Sima AAF, Zhang W, Xu G, Sugimoto K, Guberski D, Yorek MA. 2000. A comparison of diabetic polyneuropathy in type II diabetic BBZDR/Wor rats and in type I diabetic BB/Wor rats. Diabetologia 43:786–793.

Tait S, Gunn-Moore F, Collinson JM, Huang J, Lubetzki C, Pedraza L, Sherman DL, Colman DR, Brophy PJ. 2000. An oligodendrocyte cell adhesion molecule at the site of assembly of the paranodal axo–glial junction. J Cell Biol 150:657–666.

Thomas PK, Beamish NG, Small JR, King RHM, Tesfaye S, Ward JD, Tsigos C, Young RJ, Boulton AJM. 1996. Paranodal structure in diabetic sensory polyneuropathy. Acta Neuropathol 92:614–620.

Towfighi J, Gonatas N. 1977. The distribution of peroxidases in the sciatic nerves of normal and hexachlorophene intoxicated developing rats. J Neurocytol 6:39–47.

Uchikoshi F, Yang Z-D, Rostami S, Yokoi Y, Capocci P, Barker CF, Naji A. 1999. Prevention of autoimmune recurrence and rejection by adenovirus-mediated CTLA4Ig gene transfer to the panceatic graft in BB rat. Diabetes 48:652–657.

Vabnick I, Messing A, Chiu SY, Levinson SR, Schachner M, Roder J, Li CM, Novakovic S, Shrager P. 1997. Sodium channel distribution in axons of hypomyelinated and MAG null mutant mice. J Neurosci Res 50:321–336.

Vabnick I, Shrager P. 1998. Ion channel redistribution and function during development of the myelinated axon. J Neurobiol 37:80–96.

Vabnick I, Trimmer JS, Schwarz TL, Levinson SR, Risal D, Shrager P. 1999. Dynamic potassium channel distributions during axonal development prevent aberrant firing patterns. J Neurosci 19:747–758.

Wang H, Kunkel DD, Martin TM, Schwartkroin PA, Tempel BL. 1993. Heteromultimeric K^+ channels in terminal and juxtaparanodal regions of neurons. Nature 365:75–79.

Zamboni L, de Martino C. 1967. Buffered picric-acid formaldehyde: a new rapid fixative for electron-microscopy. J Cell Biol 35:148A.

Zhou L, Zhang CL, Messing A, Chiu SY. 1998. Temperature-sensitive neuromuscular transmission in Kv1.1 null mice: role of potassium channels under the myelin sheath in young nerves. J Neurosci 18:7200–7215.